

 Open access • Posted Content • DOI:10.1101/2020.09.18.300087

Combining Ancient DNA and Radiocarbon Dating Data to Increase Chronological Precision — [Source link](#)

Jakob Sedig, Nick Patterson, Iñigo Olalde, David Reich

Institutions: Harvard University, Massachusetts Institute of Technology

Published on: 18 Sep 2020 - bioRxiv (Cold Spring Harbor Laboratory)

Topics: Radiocarbon dating and Ancient DNA

Related papers:

- [Combining ancient dna and radiocarbon dating data to increase chronological accuracy.](#)
- [Empirical calibrated radiocarbon sampler: a tool for incorporating radiocarbon-date and calibration error into Bayesian phylogenetic analyses of ancient DNA](#)
- [Challenges in sample processing within radiocarbon dating and their impact in 14C-dates-as-data studies](#)
- [Cumulative probability functions and their role in evaluating the chronology of geomorphological events during the Holocene](#)
- [Building and testing age models for radiocarbon dates in Lateglacial and Early Holocene sediments](#)

Share this paper:    

View more about this paper here: <https://typeset.io/papers/combining-ancient-dna-and-radiocarbon-dating-data-to-12h6kor78u>

1 **COMBINING ANCIENT DNA AND RADIOCARBON DATING DATA TO**
2 **INCREASE CHRONOLOGICAL PRECISION**

3
4 Jakob W. Sedig^{1,2}, Iñigo Olade^{1,3}, Nick Patterson^{1,2}, David Reich^{1,2,4,5}

5
6 ¹ Department of Genetics, Harvard Medical School, Boston, MA 02115, USA.

7 ² Department of Human Evolutionary Biology, Harvard University, Cambridge, MA
8 02138, USA.

9 ³ Institute of Evolutionary Biology, CSIC-Universitat Pompeu Fabra, 08003 Barcelona,
10 Spain.

11 ⁴ Broad Institute of Harvard and MIT, Cambridge, MA 02142, USA.

12 ⁵ Howard Hughes Medical Institute, Harvard Medical School, Boston, MA 02115, USA.

13
14 Correspondence to: Jakob Sedig (Jakob_Sedig@hms.harvard.edu)

15
16
17
18 **Abstract**

19
20 This paper examines how ancient DNA data can enhance radiocarbon dating. Because
21 there is a limit to the number of years that can separate the dates of death of related
22 individuals, the ability to identify first-, second-, and third-degree relatives through
23 aDNA analysis can serve as a constraint on radiocarbon date range estimates. To
24 determine the number of years that can separate related individuals, we modeled
25 maximums derived from biological extremes of human reproduction and death ages and
26 compiled data from historic and genealogical death records. We used these estimates to
27 evaluate the date ranges of a global dataset of individuals that have been radiocarbon
28 dated and for which ancient DNA analysis identified at least one relative. We found that
29 many of these individuals could have their date ranges reduced by building in date of
30 death separation constraints. We examined possible reasons for date discrepancies of
31 related individuals, such as dating of different skeletal elements or wiggles in the

32 radiocarbon curve. Our research demonstrates that when combined, radiocarbon dating
33 and ancient DNA analysis can provide a refined and richer view of the past.

34

35 **Keywords**

36 Ancient DNA; radiocarbon dating; genealogy; Bayesian analysis

37

38

39 **1. Introduction**

40

41 This article examines how aDNA data can be used innovatively to help with a central
42 aspect of archaeological research—chronology. Ancient DNA (aDNA) data are
43 revolutionizing the field of archaeology. Within the last decade alone, aDNA analyses
44 have discovered new hominins (Reich et al., 2010), elucidated the spread of farming
45 through Europe (Lazaridis et al., 2016; Mathieson et al., 2015), shed light on the peopling
46 of the Americas and Oceania (Lipson et al., 2018; Moreno-Mayar et al., 2018; Posth et
47 al., 2018; Rasmussen et al., 2014; Skoglund et al., 2016), and more. While aDNA has
48 helped provide insight on long-standing archaeological questions, exponentially
49 increasing aDNA data has created unique opportunities for the examination of finer-
50 grained issues, and even archaeological methods.

51 The basis of the work presented here is tied to the fact that there is a maximum
52 number of years that can separate the dates of death (DOD) for two or more genetically
53 related individuals. For example, it is exceedingly rare for a mother to die 100 years
54 before her daughter, particularly in pre-modern societies. Thus, if two or more

55 individuals are identified as biological relatives through aDNA analysis and those
56 individuals are radiocarbon dated, their relatedness can be used as a prior or constraint
57 when analyzing their overlapping radiocarbon date ranges. Using these constraints, we
58 examine how the identification of genetic relatives can help identify errors and outliers in
59 radiocarbon dating, how biological relatedness can be used to constrain overlapping
60 radiocarbon date ranges and increase dating precision, and how application of the
61 methods to a large database of published ancient DNA data
62 ([https://reich.hms.harvard.edu/downloadable-genotypes-present-day-and-ancient-dna-](https://reich.hms.harvard.edu/downloadable-genotypes-present-day-and-ancient-dna-data-compiled-published-papers)
63 [data-compiled-published-papers](https://reich.hms.harvard.edu/downloadable-genotypes-present-day-and-ancient-dna-data-compiled-published-papers)) can reveal potential larger issues in the radiocarbon
64 record at particular times and places.

65

66

67 **2. Materials and Methods**

68 *2.1 Identification of genetic relatives with ancient DNA*

69

70 Identification of genetic relatives has become standard practice in ancient DNA analysis.
71 Typically, individuals which are screened and produce working genomic data are
72 compared against each other and previously analyzed individuals from similar geographic
73 regions and time periods to identify unique genetic relationships. For each pair of
74 individuals in this study, we computed the mean mismatch rate using all the autosomal
75 SNPs with at least one sequencing read for both individuals in the comparison (this
76 procedure to identify genetic relatives is described in Kennett et al. (2017:156) and van
77 de Loosdrecht et al. (2018:15), and is similar to that in Kuhn et al. (2018:157)). In the

78 cases with more than one sequencing read at a particular SNP for a given individual, we
79 randomly sample one for analysis. We then estimate relatedness coefficients as in
80 Kennett et al (2017:156): $r = 1 - ((x-b)/b)$ with x being the mismatch rate and b the base
81 mismatch rate expected for two genetically identical individuals from that populations,
82 which we estimate by computing intra-individual mismatch-rates. We also compute 95%
83 confidence intervals using block jackknife standard errors (Olalde et al., 2019:S61).
84 While such analysis can detect relationships up to the 5th degree, we limit relationships
85 here to 3rd degree maximum, as DOD date separations become too great to be of use
86 with decreasing genetic relatedness (e.g. great-grandparents and grandchildren).

87

88 *2.2 Genetic relatives and DOD separation maximums*

89

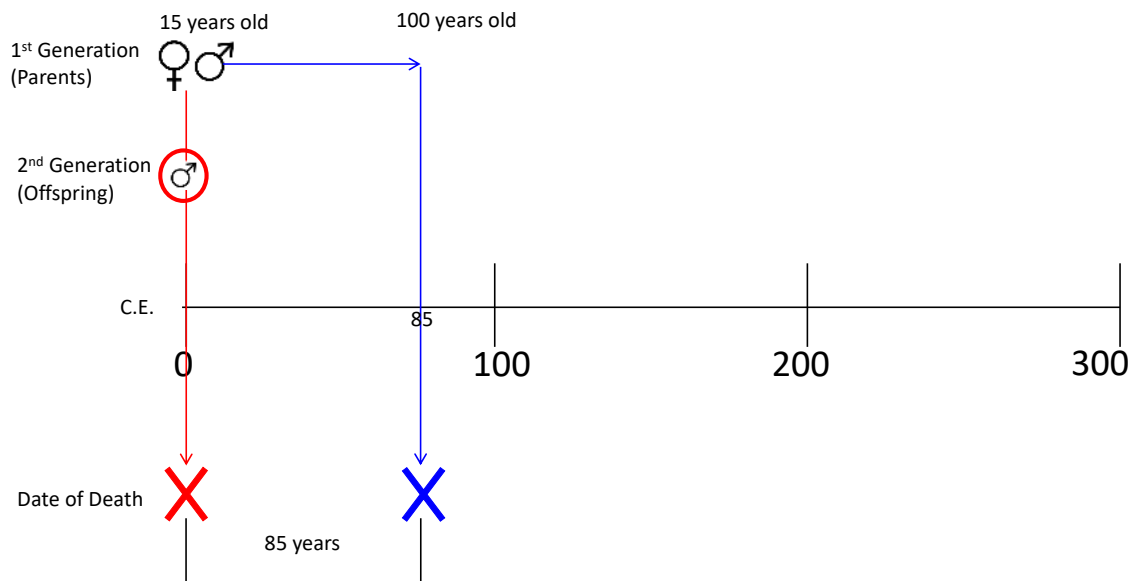
90 Below, two approaches—biological maximums and genealogically and historically
91 derived estimates—are examined for determining the DOD separation of genetically
92 related individuals. The biological maximums serve as theoretical extremes that, while
93 biologically possible, are very rare and unlikely to occur, especially in pre-industrial
94 archaeological cultures. Genealogically and historically (GH) derived DOD separations
95 were created through the examination of genealogical records and historic data and
96 reflect more realistic estimates of the number of years between the death of two related
97 individuals.

98

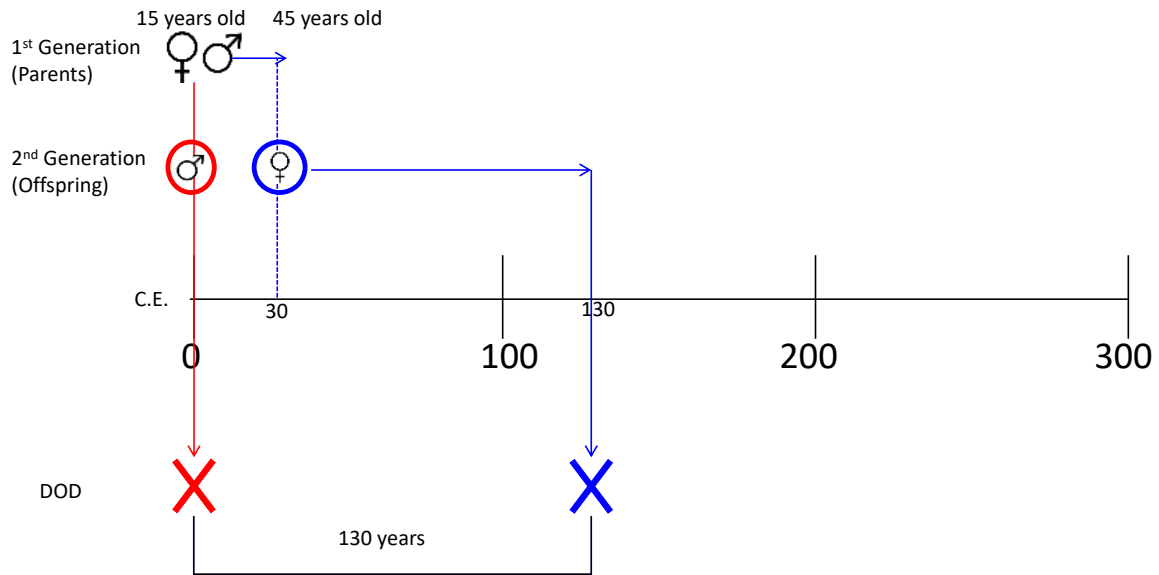
99 *2.3 Biological Maximum DOD Estimates*

100

101 Biological maximum estimates use extremes of human reproduction and lifespan to
102 produce maximum DOD separation estimates. Figures 1 and 2 (also see SM 1) are
103 diagrams of how these estimates were modeled. The start of these models is set at 0 CE.
104 At this point, a couple consisting of a 15-year-old male and female parent a male child.
105 This child dies at birth, but both parents live to be 100 years old. Thus, the DOD
106 separation between the child and parents would be 85 years. If instead the mother died
107 during childbirth, but the child lived to 100 years old, the maximum DOD separation
108 between parents-offspring would be 100 years. Siblings have an even greater potential
109 maximum DOD separation, as Figure 2 demonstrates. In this model, the 15-year-old
110 couple has a male child that dies at 0 CE. That same couple has another child 30 years
111 later (when they are 45 years old); that second child then dies 100 years later. So, the
112 maximum separation between the siblings is 130 years.



114 Figure 1. Model of biological maximum date of death separation for parents-offspring.



115

116 Figure 2. Model of biological maximum date of death separation for siblings.

117

118 Using these parameters, a number of potential biological maximums were
 119 modeled for various degrees of genetic relatedness (Table 1; see SM 1 for diagrams of
 120 models). The biological DOD maximums presented above and in Table 1 are reliant on
 121 extremes—producing children at the biologically earliest and latest possible ages and
 122 living to extreme old age. While possible, these DOD separations are not realistic, and
 123 are largely ineffective as constraints on C14 date range distributions. Thus, to more
 124 effectively examine how date of death separations for related individuals can be applied
 125 to overlapping radiocarbon ranges, we also compiled birth and death data from historical
 126 and genealogical records.

127

128

129

130

131 Table 1. Theoretical DOD separation biological maximums.

Relation	Max Years Separation
1 st (Parents-Offspring)	100
1 st (Siblings)	135
2 nd (Grandparents-Grandchildren)	180
3 rd (Cousins)	195
2 nd (Aunts/Uncles-Nieces/Nephews)	210

132

133 *2.4 Genealogically and Historically Derived DOD Estimates*

134

135 We began compiling data on the date of death separations for related individuals
136 by consulting the plethora of genealogical and historical data that are publicly available
137 online. Many of these databases consist primarily of people of European ancestry who
138 lived within the last two centuries. However, to create date of death estimates from
139 heterogenous data, we sought non-European focused databases for relatives' death dates.
140 Data were gathered from historic Anglo cemeteries, and online databases of birth and
141 death dates for Cherokee, Tlingit, and other Native American groups (SM 2). Data were
142 sorted by categories of relatedness: parent-offspring, sibling, grandparent-grandchild, and
143 other 2nd-3rd degree (aunts-uncles/nieces-nephews and cousins).

144 The DOD separation for related individuals was compiled into a spreadsheet for
145 each genealogical database (SM 2). DOD separations were calculated by identifying
146 related individuals then subtracting the dates of death (i.e. if a mother and daughter were
147 identified, and the mother died in 1800 CE and the daughter 1850 CE, the separation

148 between the two entered in the database would be 50). For parent-child and grandparent-
 149 grandchild relationships the signed value of the DOD was recorded. As will be discussed
 150 later, knowing whether the child died before the parent (which would result in a negative
 151 value) is useful for building constraints of parent-child and grandparent-grandchild
 152 radiocarbon ranges. However, since in many instances aDNA cannot determine the
 153 relatedness direction of two individuals (e.g. which is the mother and which is the
 154 daughter) the absolute value of DOD separation of each relative pair was recorded for
 155 each relationship type and is primarily used for the analyses below.

156 A total of 5235 relative DOD separations were recorded: 800 parent-offspring,
 157 813 sibling, 485 grandparent-grandchild, and 3137 other 2nd-3rd degree. The means,
 158 medians, and standard deviations of the absolute value for each relationship type were
 159 then calculated; the results are provided in Table 2 (see also SM 2).

160

161 Table 2. Compiled genealogical and historical data for DOD absolute value separation

	Parent- Offspring	Sibling	Grandparent- Grandchild	Other 2nd-3rd relationships
Mean	28.84	26.33	35.00	34.94
Median	26	20	39	30
Standard Dev.	18.94	22.41	31.93	25.6

162

163

164 The data in Table 2 demonstrate that the biologically maximum DOD separation
 165 estimates in Table 1 are truly extremes. The largest mean separation in the GH dataset
 166 was 35.00 years between grandparents-grandchildren. The single greatest DOD
 167 separation in all the data was 117 years between Cherokee 2nd/3rd degree relatives—still

168 93 years short of the 2nd/3rd degree maximum theoretical estimate (210 years). The mean
169 GH DOD separation estimates for parents-offspring, siblings, and grandparents-
170 grandchildren are 71.16, 108.67, and 145.00 less than the biological maximum separation
171 estimates (Table 1), respectively.

172 The DOD separations above were produced by manual collection from online,
173 publicly available resources. However, in a 2018 study Kaplanis and colleagues
174 developed software and an analysis pipeline to examine genealogies of millions of
175 individuals downloaded from the online genealogical database geni.com. Kaplanis et al.
176 (2018) used this data to construct family trees (sometimes containing millions of
177 individuals); the anonymized data from this study were made available to download
178 (<https://familinx.org/>). Significantly, the data contained information on which individuals
179 had parent-offspring relationships, and the death date for each individual. We therefore
180 downloaded these data and found the DOD separation for over 8 million parents and
181 offspring (SM 3). We removed pairs with data errors (for example a death date of 3500)
182 and used the biological DOD separations defined above for parent-offspring as
183 constraints (i.e. 85 years for children dying before parents and 100 years for parents
184 dying before children). The mean absolute value DOD separation for these 8 million
185 parent-offspring pairs was 31.43 years, slightly higher than the mean value we manually
186 collected (28.84; SM 2); however, this should be expected as the geni.com data is heavily
187 weighted toward modern, European individuals who likely had longer life spans. Overall,
188 the similarity between the Kaplanis et al. 2018 data and the genealogical and historical
189 data we manually curated demonstrates that the DOD separations we obtained represent
190 more realistic DOD separations for related individuals than the biological maximums.

191 Although the DOD separation estimates derived from GH data are more reflective
192 of separations between genetic relatives than the biologically possible maximums, the
193 GH data presented here should be viewed only as rough estimates. More precise
194 estimates could be tailored for particular types of social organization, such as hunter-
195 gatherers, pastoralists, agriculturalists, city-dwellers, nomads, etc. However, should
196 researchers wish to create new models, the GH estimates above likely will not be
197 exceeded, as many of the separations were derived from individuals who lived after the
198 industrial revolution and likely had longer lifespans than ancient individuals.

199

200

201 **3. Application and analysis**

202 *3.1 Applications of relatedness data to radiocarbon dated individuals*

203

204 We examined the ancient DNA database of published individuals from geographic
205 locales across the globe spanning more than 30,000 years (although there is bias towards
206 the last 10000 years in western Eurasia; see Marciniak and Perry, 2017; Reich, 2018) to
207 test how DOD separation estimates can be applied to related individuals and examine if
208 any new insights can be revealed. As of May 2020, 3,965 published individuals were in
209 the database, with 1,127 ancient individuals having at least one identified relative. Of
210 those, 190 pairs (231 unique individuals, SM 4) had both individuals C14 dated (all dates
211 generated with AMS and calibrated two-sigma), allowing for analysis of DOD
212 separations and constraints.

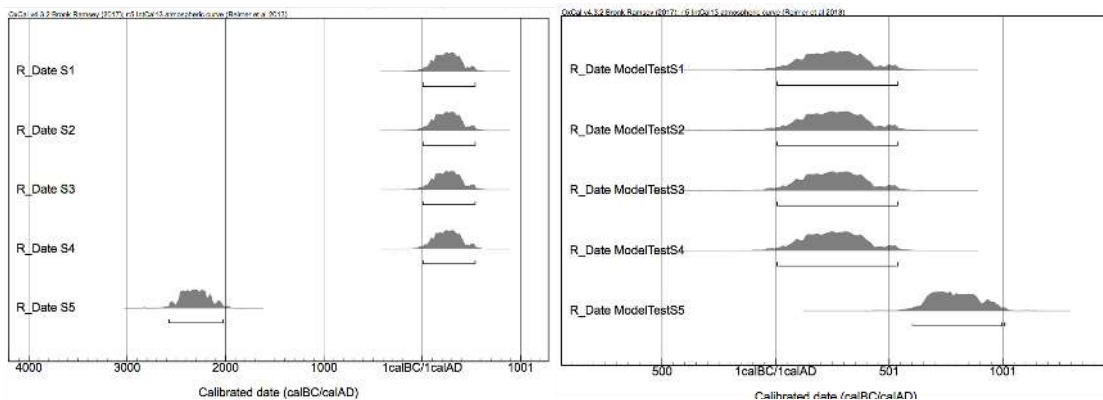
213

214 3.2 Outlier identification

215

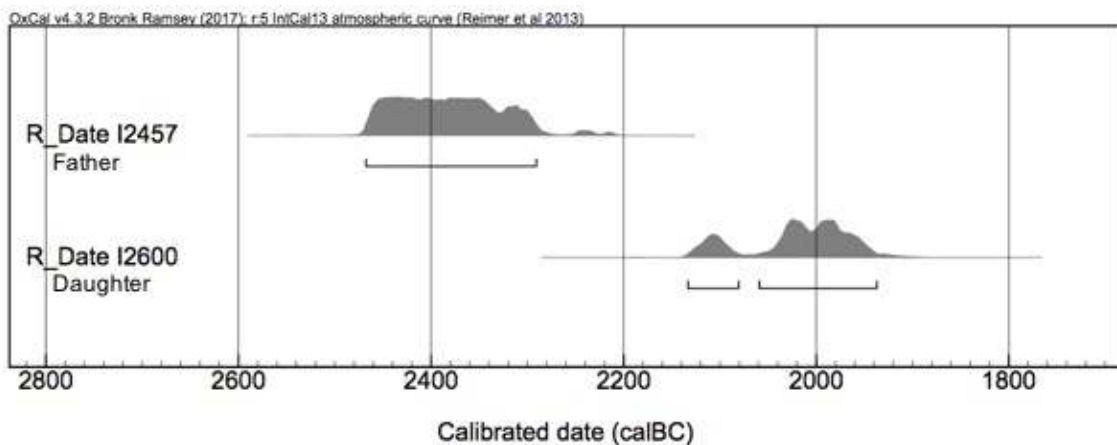
216 The most basic example of how genetic relatedness can help refine radiocarbon dating is
217 through the identification of anomalies. Archaeologists have long recognized that C14
218 sample contamination can occur and that other issues, such as the marine reservoir effect,
219 can cause dates to be skewed (Taylor and Bar-Yosef, 2014). Genetic relatedness is a new
220 independent measurement that can be used to test the validity of radiocarbon date ranges,
221 particularly for samples that might not be obvious outliers. For example, if five skeletons
222 from the same stratigraphic layer in a cemetery were dated, and four of those individuals
223 had calibrated ranges of approximately CE 1-500, while one had a calibrated date range
224 of approximately 2500-2000 BCE, that one sample would seem suspicious and would
225 likely be redated (Figure 3). However, if that outlier instead had a range of approximately
226 CE 600-1000, the skeleton might not be redated, as it is relatively close to the range of
227 the other four skeletons (Figure 3). But, if it was determined that the outlier was actually
228 the father of skeleton 3, then it would be highly suspicious that skeleton 5 could be older
229 than skeleton 3, as the DOD separation between father and offspring cannot biologically
230 be more than 100 years, and more realistically is around 29 years from GH DOD
231 estimates (Table 1). Such an example was discovered in the database.

232



233 Figure 3. Examples of clear outliers in radiocarbon dating (L) and an individual that is an
234 outlier but does have overlap with other dates (R).
235

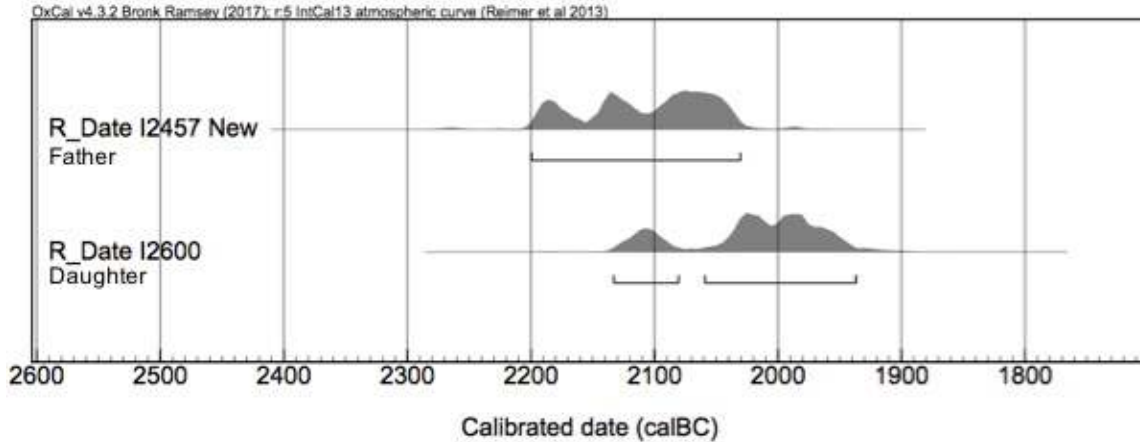
236 Two individuals, I2457 and I2600 (Olalde et al., 2018), were excavated from two
237 sites, Amesbury Down and Porton Down, Britain, separated by approximately 5km. The
238 samples had been previously radiocarbon dated; prior to aDNA analysis and the dates did
239 not seem suspect (I2457= 3890 \pm 30; 2480-2280 calBCE, SUERC-36210;
240 I2600=3646 \pm 27; 2140-1940 calBCE, SUERC-43374; Figure 4). Ancient DNA analysis
241 of the samples revealed that I2600 was the daughter of I2457, but there was thus no
242 overlap in the calibrated distributions of the father-daughter pair. The minimum DOD
243 separation between the father and daughter was 140 years, which exceeds even maximum
244 biological estimates. Individual I2457 (the father) was therefore redated and the new date
245 (3717 \pm 28; 2200-2031 calBCE; SUERC-69975) fit within the expected DOD spread
246 (Figure 5).
247



248
249 Figure 4. Original AMS dates for I2457 and I1600.

250

251



252

253 Figure 5. New AMS date for I2457.

254

255 *3.3 Range tightening of radiocarbon date distributions*

256

257 Along with detecting outliers, we examined the potential of using DOD separations to

258 refine calibrated date ranges in instances where two (or more) related individuals with

259 overlapping C14 date probability distribution ranges are identified. Using biological

260 maximums as an example, consider a father whose AMS range is 1-500 calCE and a

261 daughter whose range is 400-1000 calCE. Since the father cannot have died more than

262 100 years before or after the daughter, the father's range can be constrained to

263 approximately 300-500 CE; since the daughter cannot have died more than 100 years

264 after the father, the daughter's range can be constrained to 400-600 CE.

265 While informative for some related pairs, the maximum biological separation

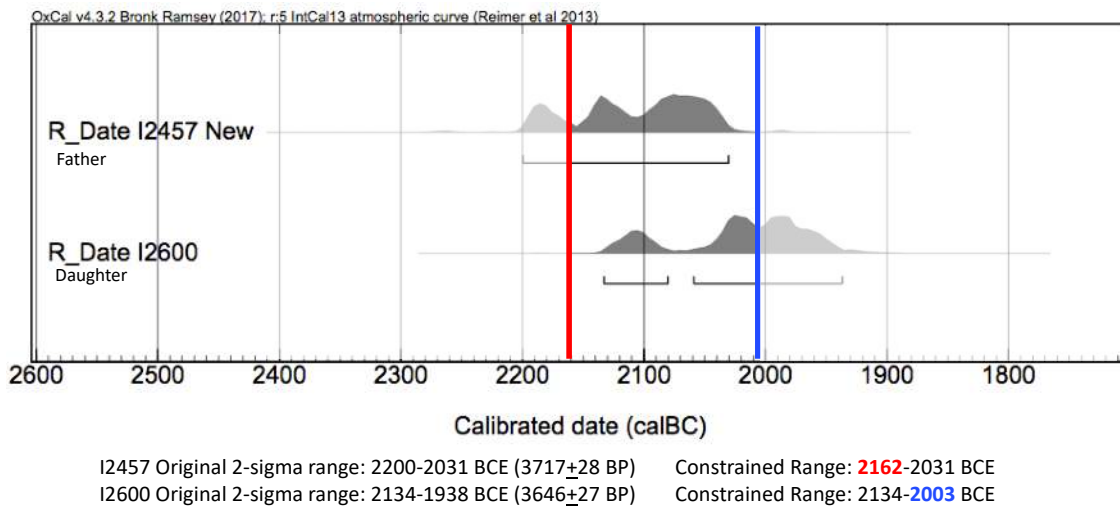
266 estimate is often too large and not applicable to most related and dated individuals in the

267 dataset. Individuals I2457 and I2600 serve as examples of how GH DOD separations can

268 be used as constraints for the date ranges of related individuals. Using the new date for

269 I2457 and building in the 29-year parent-offspring GH DOD constraint allows the

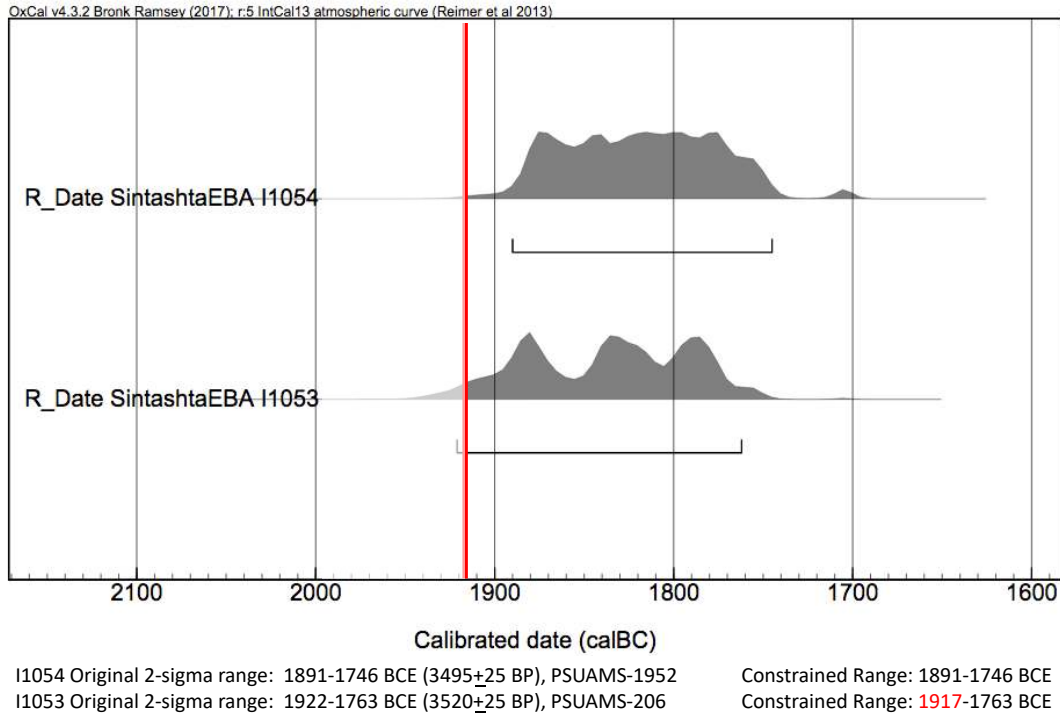
270 individual and combined date ranges to be reduced (Figure 6). With this estimate, the tail
 271 ends of the calibrated distributions for I2457 and I2600 should not be separated by more
 272 than 29 years. In other words, since I2457 likely died an average of 29 years before
 273 I2600, adding 29 years to the left end of the two-sigma calibrated date range for I2600,
 274 2134 BCE, creates a constraint for the earliest date of I2457 at 2163 BCE. On the other
 275 end of the distributions, since I2600 likely did not die more than 29 years after I2457,
 276 adding 29 years to the latest dates of the 2-sigma calibrated range of I2457, 2031 BCE,
 277 creates a constraint for the latest date of I2600 at 2002 BCE (Figure 6).
 278



279
 280 Figure 6. AMS ranges for I2457 and I2600 with relative constraints added.

281
 282 Not all date ranges can be constrained as significantly as with these relatives, as
 283 demonstrated by individuals I1054 and I1053 (Narasimhan et al., 2019), two siblings
 284 from the Russian Sintashta archaeological culture. Their date ranges overlap almost
 285 entirely (Figure 7). Thus, using the 26-year GH DOD separation estimate for siblings,

286 only a minor reduction can be made for their individual and combined 2-sigma date
287 ranges (a change in only two years).



288

289 Figure 7. AMS ranges for I1054 and I1053 with relative constraints added.

290

291 3.4. Constraints applied to database

292

293 We applied the date range distribution tail trimming approach outlined above to the 190
294 dated relative pairs in the database (we used separations of 29 years for parent-offspring,
295 26 for siblings, and 35 years for 2nd-3rd degree of unknown specificity as constraints).

296 We focus below on GH DOD derived constraints, as the biologically maximal DOD
297 constraints often exceeded the overlap of the related pairs' C14 distributions. As

298 mentioned above, since the type and directionality of relationships often cannot be

299 precisely determined through aDNA analysis, we used the largest mean absolute values

300 for DOD separations derived from GH data. In other words, if a pair could only be
 301 distinguished as 1st degree relatives (either parent-offspring or siblings), the largest mean
 302 GH DOD separation for first degree relatives was used, which is 29 years (for parent-
 303 offspring, not 26 years for siblings).

304 After applying GH DOD constraints to the dataset, we removed 21 pairs because
 305 their 2-sigma calibrated date ranges did not overlap and exceeded the GH DOD
 306 estimates, suggesting dating error/a need for redating (uncorrected marine reservoir
 307 effect, sample contamination, etc). This left a total of 169 pairs and 219 unique
 308 individuals (SM 4). Applying the GH constraints, we were able to reduce the 2-sigma
 309 calibrated ranges of 132 individuals, with a mean reduction of 54.47 years (Table 3 and
 310 SM 4.2); 77 individuals had even more of a reduction than this. Figure 8 is a graph of the
 311 difference between the original 2-sigma calibrated range and the GH constrained range
 312 for each individual.

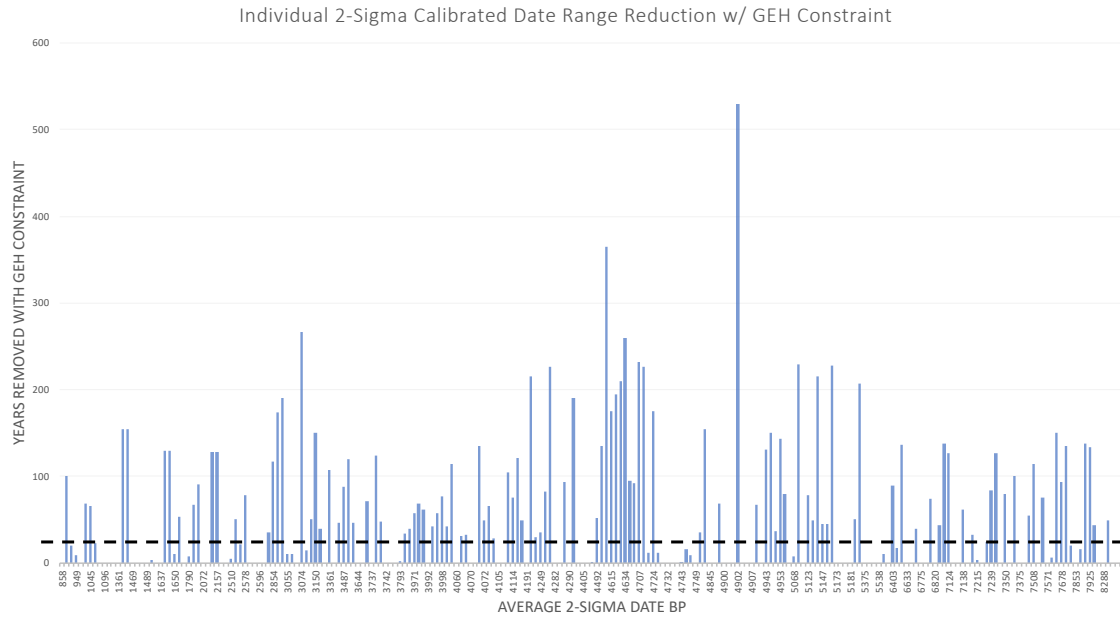
313

314 Table 3. Date ranges for all individuals in relative pairs.

	Original Range¹	GH Range²	(O)- (GH) Change³
Mean	203.44	149.00	54.47
Standard Deviation	95.89	86.60	75.82

315 ¹Original range is the 2-sigma calibrated range for the individual. ²GH range builds in the
 316 constraints derived from ethnographic/historic records for each individual (Table 2).

317 ³(O)-(GH) Change is the original range minus the constrained biological range for each
 318 individual, which reveals how many years of the original range are removed from the tail
 319 ends of the 2-sigma distributions when GH estimate constraints are applied.



320

321 Figure 8. Difference between original 2 sigma calibrated date range and GH constrained
 322 range for all 219 individuals, ordered from most recent date BP to oldest.

323

324 One possible reason for large date range reductions is if different skeletal
 325 elements were radiocarbon dated for each individual in the relative pairs. Studies have
 326 demonstrated that different skeletal elements have different rates of remodeling and
 327 carbon uptake (Calcagnile et al., 2013; Cook et al., 2015; Hansen et al., 2017; Pinhasi et
 328 al., 2015); for example, a long bone (tibia, femur, etc.) remodels throughout an
 329 individual’s life and therefore regularly uptakes new carbon, whereas the otic capsule
 330 completes formation in utero and does not remodel during an individual’s lifetime. Thus,
 331 if a femur and otic capsule from the same individual are radiocarbon dated, two different
 332 dates may be generated, particularly in advanced-age individuals. This could potentially
 333 lead to discrepant date ranges for related individuals—if the otic capsule of an adult
 334 female who died giving childbirth was dated, while the femur of her daughter was used,
 335 there could in theory be a difference of more than 100 years. We therefore compiled data

336 on which element of each individual was radiocarbon dated; information on which
337 skeletal element was radiocarbon dated for each individual is provided in SM 4.1.
338 Unfortunately, in many instances no information on which element was dated was
339 available in the published literature. Additionally, if information was provided, it was
340 sometimes imprecise or vague. An element might be listed as “petrous”, but with no
341 information on if the otic capsule, cochlea, or ossicles were radiocarbon dated—these
342 could generate earlier dates than the surrounding petrous pyramid or temporal bone.

343 We hypothesized that there would be a higher number of individuals above the
344 54.47 GH mean reduction for individuals in a related pair that had different skeletal
345 elements C14 dated. Table 4 provides counts of whether the skeletal element dated for
346 each individual was different or the same (or if no information was available) as their
347 relative. While there does seem to be a higher proportion of individuals with reductions
348 above the 54.47 year GH mean in instances where different elements were radiocarbon
349 dated, this is not statistically significant (chi-square test; $x^2=1.96$, p value= 0.3755, df=2;
350 SM 4.4), suggesting that dating different elements of related pairs does not significantly
351 impact the reductions made with GH constraints. This likely is due to the fact that despite
352 different elements being dated, most relatives were relatively close in age (likely because
353 few individuals in pre-modern societies reached advanced age), or that the different
354 elements dated had similar bone remodeling/carbon uptake rates. Despite this, it is likely
355 that some instances of large discrepancies can be explained by the C14 dating of different
356 skeletal elements.

357

358 Table 4. Counts and percentage of whether the same or different skeletal elements were
359 used to date an individual in a relative pair.

360

Comparison of skeletal element dated for each related pair	N individuals	% above 54.47 year mean GH reduction per element category
Different elements	26	50.0
Same element	138	30.9
No information available	55	34.1

361

362

363

364

365

366

367

368

369

370

371

372

373

374

375

376

377

378

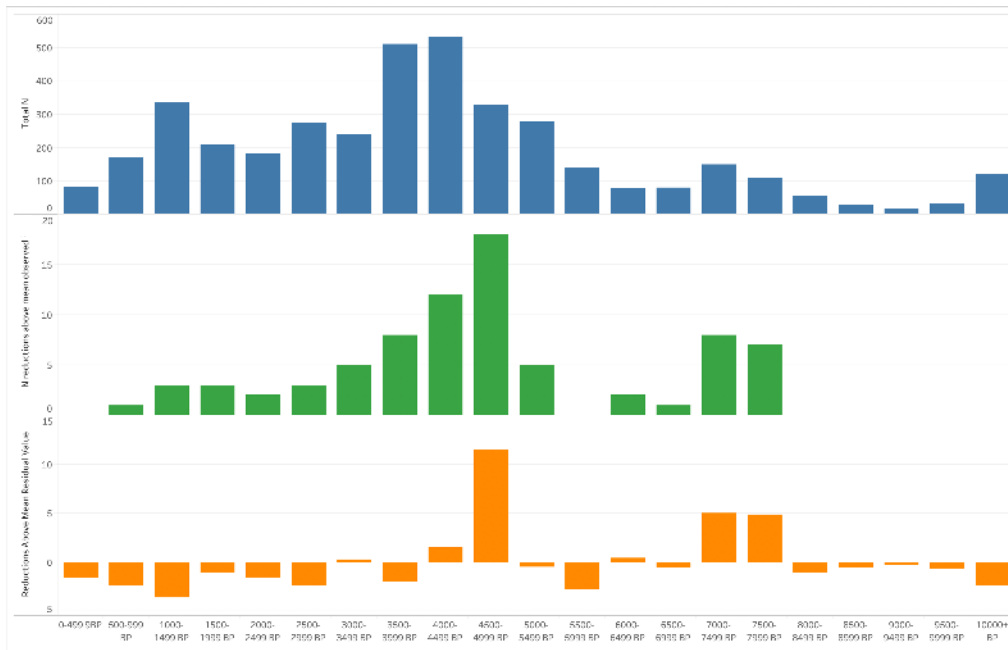
379

We next examined whether applying GH constraints could reveal larger patterns in the dataset. To explore if there were any periods which had a higher number of relatives that exceeded the mean reduction than others, we binned into 500-year intervals all 3965 published individuals in the database and the 219 dated individuals with genetically identified relatives. This allowed us to examine if periods with high numbers of individuals above the 54.47 year mean GH reduction were indicative of anomalies in the radiocarbon record (i.e. calibration curve issues, uncorrected marine reservoir effects, etc) at a particular date interval, or merely an artifact of sampling the database. Figures 9a and 9b qualitatively demonstrate that periods with a high number of individuals with a reduction above the 54.47 year mean roughly corresponds with the 500-year intervals that have been most densely sampled for aDNA. We performed a χ^2 test to test the null hypothesis that the number of individuals above the 54.47 year mean GH reductions per 500-year interval correlates with the total number of individuals sampled per 500-year interval. We found a χ^2 value of 57.43 (df=20), giving a p value= 1.76717E-05 (SM 4.5), rejecting the null hypothesis and suggesting that the number of individuals above the 54.47 mean GH reduction per 500-year interval is not simply due to the overall number of individuals sampled per 500-year interval. The most notable intervals were 7999-7500

380 BP, 7499-7000 BP, 4999-4500 BP, and 4499-4000 BP (Figure 9.C), which had residual
 381 values of 4.86, 5.07, 11.59, and 1.65, respectively (SM 4.5).

382

383



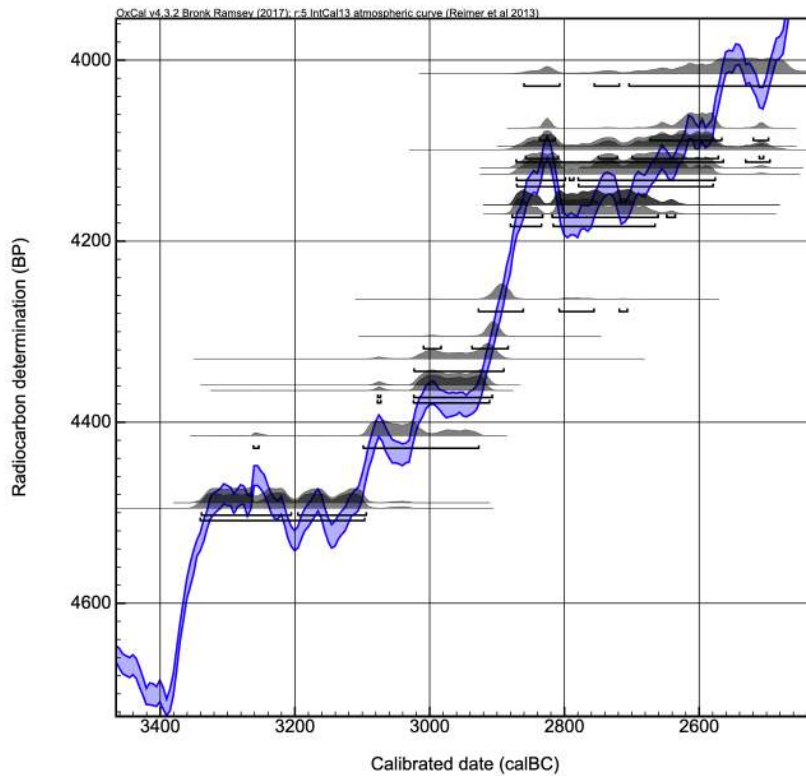
384

385 Figure 9. Data from the database and 219 individuals with relatives binned in 500-year
 386 intervals. A) #of individuals total in each 500-year interval. B) # of relatives per interval
 387 that exceed the 54.47-year mean GH reduction C) Residuals from x^2 test.
 388

389 The 500-year interval with the most individuals that had range reductions above
 390 the 54.47-year mean (n=18) was 4999-4500 calBP. The plotted radiocarbon distributions
 391 of these individuals demonstrate that plateaus along the radiocarbon curve during this
 392 period of time could account for the high number of reductions (Figs 10), which is also
 393 true for the other three 500-year intervals with the highest x^2 residual values (Figs 11-13).

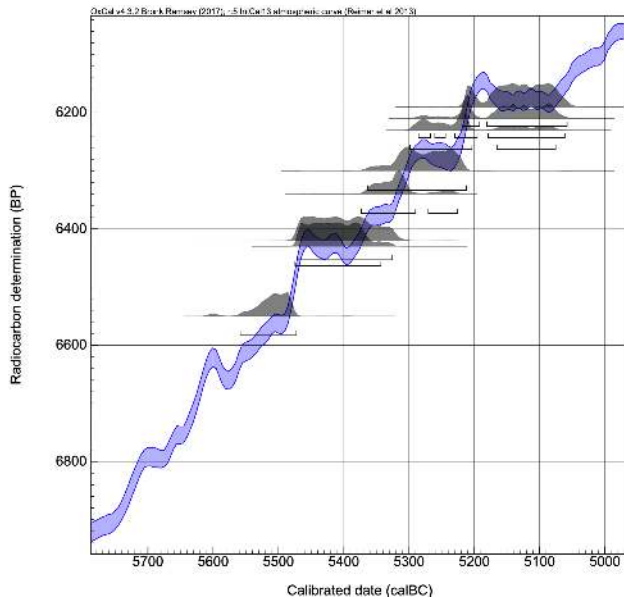
394 Individuals MX188 and MX190, 1st degree relatives from Spreitenbach,
 395 Switzerland (Furtwangler et al. 2020), demonstrate how knowing genetic relatedness and
 396 applying GH constraints can reduce date ranges and help correct for radiocarbon

397 plateaus. MX 190's 2-sigma range falls on a curve plateau and is much larger than MX
398 188's (Figure 14; 2861-2342 calBCE, ETH-19935 and 2495-2399 calBCE, BE-7995.1.1,
399 respectively). However, because these individuals are known to be 1st degree relatives the
400 29 year GH constraint could be applied, reducing MX 190's range by 365 years (to 2524-
401 2370 calBCE, SM 4.1).
402



403

404 Figure 10. Original 2-sigma calBCE date ranges for individuals from the 4500-4999
405 calBP interval that had GH reductions about the 54.47 mean.
406

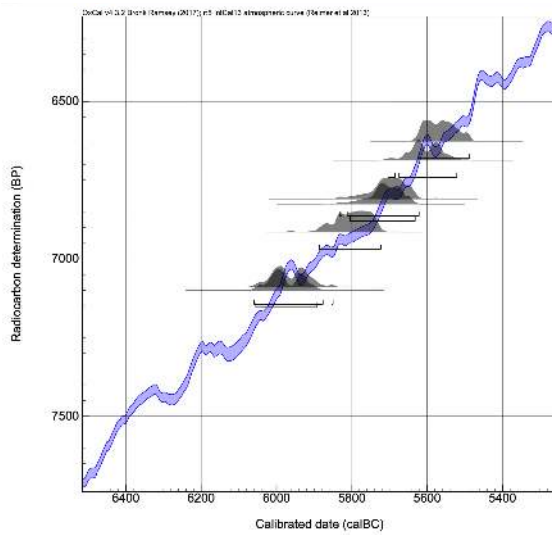


407

408 Figure 11. Original 2-sigma calBCE date ranges for individuals from the 7499-7000
 409 calBP interval that had GH reductions about the 54.47 mean.

410

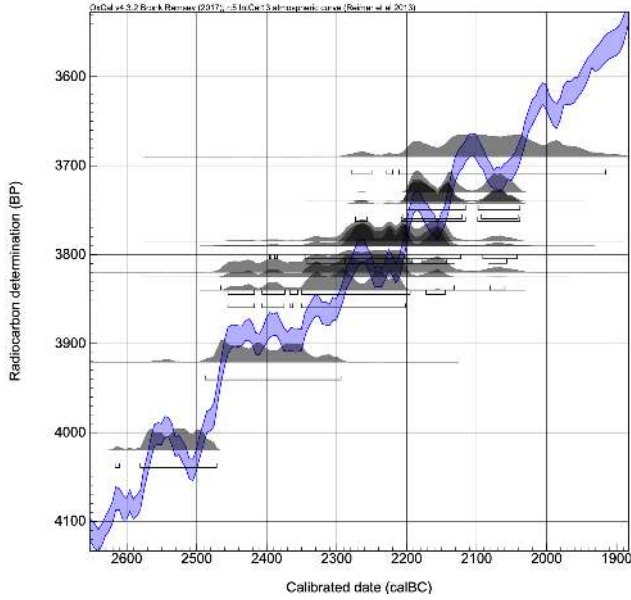
411



412

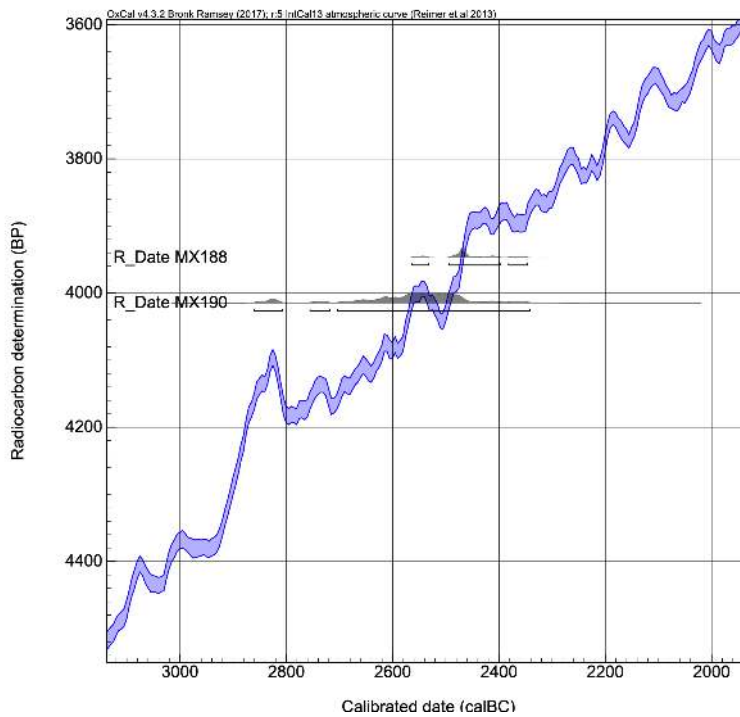
413 Figure 12. Original 2-sigma calBCE date ranges for individuals from the 7500-7999
 414 calBP interval that had GH reductions about the 54.47 mean.

415



416

417 Figure 13. Original 2-sigma calBCE date ranges for individuals from the 4000-4499 BP
 418 calBP interval that had GH reductions about the 54.47 mean.
 419



420

421 Figure 14. Original 2-sigma calBCE date ranges for MX 188 and MX 190.

422

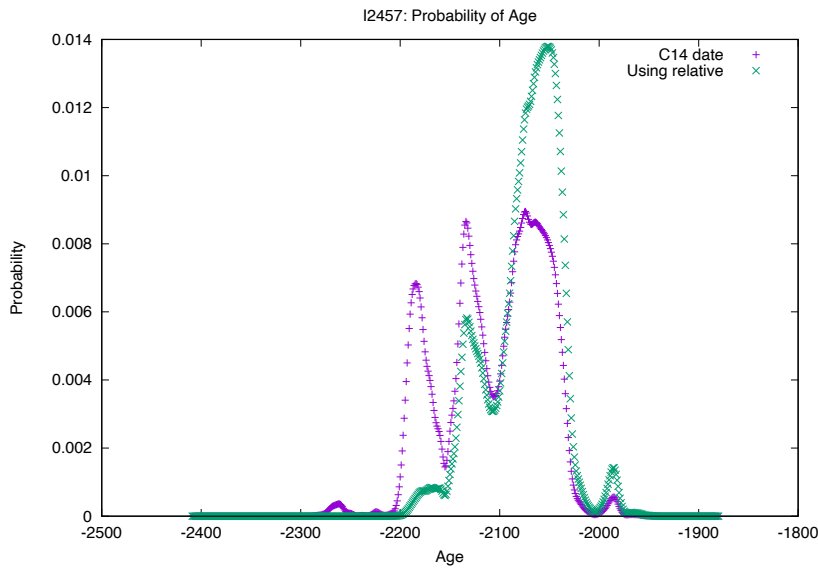
423 *3.6 Building Bayesian Models*

424

425 The range tightening described above is a “manual” method for constraining the tail ends
426 of radiocarbon date distributions using estimates for the number of years that can separate
427 the dates of death of genetic relatives. While date ranges can be constrained with this
428 manual method, we also tested how other statistical modeling could refine the date
429 ranges. Bayesian analysis to increase precision in a series of radiocarbon dates has
430 become standard practice amongst archaeologists (Bronk Ramsey, 2009; Taylor and Bar-
431 Yosef, 2014). Thus, we examined how effective knowledge of genetic relatedness and
432 date of death estimates are as priors to refine radiocarbon dates.

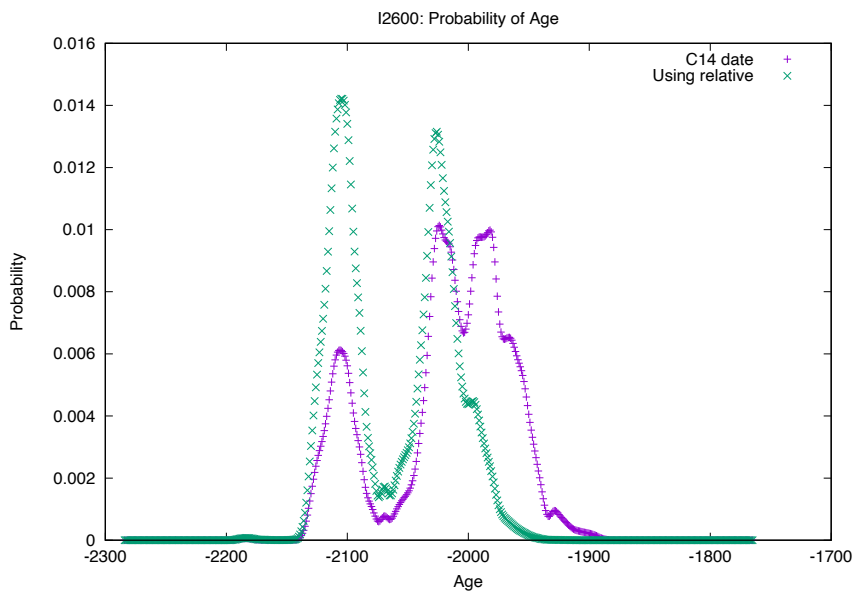
433 To test this, we started by importing the raw calibrated date probability
434 distributions for I2600 and I2457 from OxCal 4.3 (data provided in SM 5). We next
435 sorted the GH DOD values into 5-year intervals and produced a probability distribution.
436 The raw data were smoothed to give estimates of DOD by year (SM 5). The posterior
437 joint distribution of the datasets was then computed. Figures 15 and 16 are the marginal
438 estimates of these distributions for the father and daughter. Due to a plateau in the
439 radiocarbon curve, the date distributions for the father and daughter are bimodal with an
440 additional, lower probability “peak” (demonstrated with the purple curve). For each,
441 building in the relative information significantly reduces the probability of one of the
442 original probability peaks. And while the distribution for I2600 essentially remains
443 bimodal, the most likely probability for both I2600 and I2457 is between 2100-2000
444 BCE. This result demonstrates that building the constraints in to statistical modeling can
445 help refine date ranges. Future work building these constraints into Bayesian modeling
446 available in OxCal could provide additional refinements.

447



448

449 Figure 15. Joint probability distribution for I2457. Original AMS date probability
450 distribution in purple, new joint distribution in green.



451

452 Figure 16. Joint probability distribution for I2600. Original AMS date probability
453 distribution in purple, new joint distribution in green.

454

455 3.7. Summary

456

457 In sum, knowledge of genetic relatedness can be used to constrain radiocarbon date
458 distributions, either by applying DOD separations to the tail ends of the distributions, or
459 through Bayesian modeling. These refinements are not universally applicable; related
460 pairs often have date distributions that overlap, sometimes almost entirely, limiting the
461 extent to which DOD estimates can refine date ranges. Yet, overlap is what *should* be
462 expected; related individuals should not have large date separations. Date distributions of
463 related individuals that do not overlap could reveal an error in radiocarbon dating (such
464 as I2600 and I2457) or genetic analysis, or other issues, such as an uncorrected marine
465 reservoir effect. In other words, the more substantially DOD separation estimates can
466 constrain C14 date ranges, the more likely a significant issue exists in dating for any of a
467 variety of reasons (unaccounted marine reservoir effect, curve plateau, etc).

468

469

470 **4. Discussion**

471

472 Combining previously independent lines of data—knowledge of genetic relatedness
473 derived from ancient DNA; biological and estimated DOD separations for relatives; and
474 radiocarbon dates—creates potential benefits for researchers examining the ancient past.
475 Perhaps the most apparent is evaluation of data generated through disparate methods. As
476 discussed above, relatedness often confirms radiocarbon dates (and vice-versa, Saag et
477 al., 2019:5). Using genetic relatedness and DOD separation estimates to evaluate
478 radiocarbon dates can also help attend to some of the most common pitfalls in
479 radiocarbon dating. According to Taylor and Bar-Yosef (2014:132), “the most common

480 reason why C14 dating evidence is considered to be anomalous can be traced to failures
481 to clearly establish and document the physical relationship between a C14 dated sample
482 and a specific targeted event or cultural expression.” Somewhat counterintuitively,
483 incorporating genetic relationship DOD-separations addresses Taylor and Bar-Yosef’s
484 concerns by circumventing taphonomic processes. Instead of focusing on potential
485 confounding factors of when individuals were buried, removed, reburied, etc., date ranges
486 are examined with an independent line of evidence that is not prone to contamination
487 issues associated with taphonomic processes and archaeological context.

488 Analyzing the radiocarbon record with knowledge of genetic relatives also
489 provides archaeologists an opportunity to move beyond traditional interpretations of
490 radiocarbon dates. C14 dating of skeletal remains typically provides an estimate of when
491 an individual died (although it could also reflect when a particular element ceased carbon
492 uptake during an individual’s lifetime, as discussed above). The combined and
493 constrained date ranges discussed above provide minimum and maximum boundaries of
494 when two related individuals died; therefore, the overlap of the two ranges likely contains
495 the plausible period of time when the individuals were *alive* together. It is entirely
496 possible, of course, that one individual died at the minimum boundary and the other at the
497 maximum. In such instances the two related individuals would have no lifetime overlap.
498 Even in such cases, considering the combined C14 ranges of related individuals can turn
499 archaeological thinking away from incipient or terminal dates of archaeological periods,
500 but instead toward changes that happened during lifetimes.

501 Considering lifespan ranges also helps elucidate cultural plasticity, and reveal the
502 arbitrariness of archaeological boundaries. Archaeologists had initially suspected the

503 English Bell Beaker father-daughter pair were part of separate archaeological cultures
504 due to their initial dates. Knowing that these two individuals were related not only helped
505 in identifying an error in the initial radiocarbon dates, but also speaks to the subjective
506 nature of chronological and cultural boundaries archaeologists establish, which were of
507 no consequence for the father-daughter pair.

508 The approaches outlined above represent only a small number of applications for
509 how knowledge of genetic relatedness can help with radiocarbon dating. The potential for
510 further applicability needs to be explored; one promising application could be the use of
511 extended families for radiocarbon curve “wiggle matching.”

512

513

514 **5. Conclusion**

515

516 This research is a first step in combining two discrete analytical methods to add
517 refinement to interpretation of the archaeological record and is meant to demonstrate that
518 knowledge of genetic relatedness can be used to augment radiocarbon dating. As ancient
519 DNA databases continue to grow, and more relatives are identified and radiocarbon
520 dated, researchers will likely feel compelled to refine GH and DOD estimates as they see
521 fit, as some have already done (Kennett et al., 2017; Saag et al., 2019). Levels of social
522 organization (e.g. hunter-gatherer vs. agriculturalist), age of skeletons (adult vs. juvenile),
523 and lifespan estimate could also all be incorporated into estimates. Additionally, once
524 enough related individuals are identified and dated, specific regions, sub-regions, or even
525 sites can be examined for anomalies in the associated radiocarbon records.

526 Ancient DNA innovations are providing archaeologists with unprecedented
527 insight into the past. As ancient DNA becomes increasingly integral to archaeological
528 studies, researchers should explore novel applications of genetic data to archaeological
529 studies. This paper used ancient DNA to identify radiocarbon outliers, refine date
530 distribution ranges for related pairs, and delineate potential issues unaccounted for in the
531 radiocarbon record of particular eras and locales. Such studies should help integrate the
532 two fields and move ancient DNA and archaeology forward together into the next era of
533 research on the human past.

534

535 **Declaration of Competing Interests**

536 None

537

538 **Acknowledgements**

539 This work was funded by NIH grant GM100233, the Paul Allen Foundation, John
540 Templeton Foundation (grant number 6122), and David Reich is an Investigator of the
541 Howard Hughes Medical Institute. We thank Melissa Gymrek for providing assistance
542 with familinx data from the Kaplanis et al. 2018 study, Greg Hodgins for reviewing an
543 early draft of the paper, Iain Mathieson and Vagheesh Narasimhan for statistical
544 assistance, and members of our laboratory for feedback on the study during its
545 development.

546

547

548

549

550

551

552
553
554
555
556
557
558
559
560
561
562
563
564
565
566
567
568
569
570
571
572
573
574
575
576
577
578
579
580
581
582
583
584
585
586
587
588
589
590
591
592
593
594
595
596
597

References Cited

Bronk Ramsey, C., 2009. Bayesian Analysis of Radiocarbon Dates. *Radiocarbon* 51, 337–360. <https://doi.org/10.1017/S0033822200033865>

Calcagnile, L., Quarta, G., Cattaneo, C., D’Elia, M., 2013. Determining ¹⁴C Content in Different Human Tissues: Implications for Application of ¹⁴C Bomb-Spike Dating in Forensic Medicine. *Radiocarbon* 55, 1845–1849. <https://doi.org/10.1017/S003382220004875X>

Cook, G.T., Ainscough, L.A.N., Dunbar, E., 2015. Radiocarbon Analysis of Modern Skeletal Remains to Determine Year of Birth and Death—A Case Study. *Radiocarbon* 57, 327–336. https://doi.org/10.2458/azu_rc.57.18394

Hansen, H.B., Damgaard, P.B., Margaryan, A., Stenderup, J., Lynnerup, N., Willerslev, E., Allentoft, M.E., 2017. Comparing Ancient DNA Preservation in Petrous Bone and Tooth Cementum. *PLOS ONE* 12, e0170940. <https://doi.org/10.1371/journal.pone.0170940>

Kaplanis, J., Gordon, A., Shor, T., Weissbrod, O., Geiger, D., Wahl, M., Gershovits, M., Markus, B., Sheikh, M., Gymrek, M., Bhatia, G., MacArthur, D.G., Price, A.L., Erlich, Y., 2018. Quantitative analysis of population-scale family trees with millions of relatives. *Science* 360, 171–175. <https://doi.org/10.1126/science.aam9309>

Kennett, D.J., Plog, S., George, R.J., Culleton, B.J., Watson, A.S., Skoglund, P., Rohland, N., Mallick, S., Stewardson, K., Kistler, L., LeBlanc, S.A., Whiteley, P.M., Reich, D., Perry, G.H., 2017. Archaeogenomic evidence reveals prehistoric matrilineal dynasty. *Nature Communications* 8, 14115. <https://doi.org/10.1038/ncomms14115>

Kuhn, J.M.M., Jakobsson, M., Günther, T., 2018. Estimating genetic kin relationships in prehistoric populations. *PLOS ONE* 13, e0195491. <https://doi.org/10.1371/journal.pone.0195491>

Lazaridis, I., Nadel, D., Rollefson, G., Merrett, D.C., Rohland, N., Mallick, S., Fernandes, D., Novak, M., Gamarra, B., Sirak, K., Connell, S., Stewardson, K., Harney, E., Fu, Q., Gonzalez-Forbes, G., Jones, E.R., Roodenberg, S.A., Lengyel, G., Bocquentin, F., Gasparian, B., Monge, J.M., Gregg, M., Eshed, V., Mizrahi, A.-S., Meiklejohn, C., Gerritsen, F., Bejenaru, L., Blüher, M., Campbell, A., Cavalleri, G., Comas, D., Froguel, P., Gilbert, E., Kerr, S.M., Kovacs, P., Krause, J., McGettigan, D., Merrigan, M., Merriwether, D.A., O’Reilly, S., Richards, M.B., Semino, O., Shamoon-Pour, M., Stefanescu, G., Stumvoll, M., Tönjes, A., Torroni, A., Wilson, J.F., Yengo, L., Hovhannisyanyan, N.A., Patterson, N., Pinhasi, R., Reich, D., 2016. Genomic insights into the origin of farming in the ancient Near East. *Nature* 536, 419–424. <https://doi.org/10.1038/nature19310>

Lipson, M., Skoglund, P., Spriggs, M., Valentin, F., Bedford, S., Shing, R., Buckley, H., Phillip, I., Ward, G.K., Mallick, S., Rohland, N., Broomandkhoshbacht, N., Cheronet, O., Ferry, M., Harper, T.K., Michel, M., Oppenheimer, J., Sirak, K., Stewardson, K., Auckland, K., Hill, A.V.S., Maitland, K., Oppenheimer, S.J., Parks, T., Robson, K., Williams, T.N., Kennett, D.J., Mentzer, A.J., Pinhasi, R.,

598 Reich, D., 2018. Population Turnover in Remote Oceania Shortly after Initial
599 Settlement. *Current Biology* 28, 1157-1165.e7.
600 <https://doi.org/10.1016/j.cub.2018.02.051>

601 Marciniak, S., Perry, G.H., 2017. Harnessing ancient genomes to study the history of
602 human adaptation. *Nature Reviews Genetics* 18, 659–674.
603 <https://doi.org/10.1038/nrg.2017.65>

604 Mathieson, I., Lazaridis, I., Rohland, N., Mallick, S., Patterson, N., Roodenberg, S.A.,
605 Harney, E., Stewardson, K., Fernandes, D., Novak, M., Sirak, K., Gamba, C.,
606 Jones, E.R., Llamas, B., Dryomov, S., Pickrell, J., Arsuaga, J.L., de Castro,
607 J.M.B., Carbonell, E., Gerritsen, F., Khokhlov, A., Kuznetsov, P., Lozano, M.,
608 Meller, H., Mochalov, O., Moiseyev, V., Guerra, M.A.R., Roodenberg, J., Vergès,
609 J.M., Krause, J., Cooper, A., Alt, K.W., Brown, D., Anthony, D., Lalueza-Fox, C.,
610 Haak, W., Pinhasi, R., Reich, D., 2015. Genome-wide patterns of selection in 230
611 ancient Eurasians. *Nature* 528, 499–503. <https://doi.org/10.1038/nature16152>

612 Moreno-Mayar, J.V., Vinner, L., de Barros Damgaard, P., de la Fuente, C., Chan, J.,
613 Spence, J.P., Allentoft, M.E., Vimala, T., Racimo, F., Pinotti, T., Rasmussen, S.,
614 Margaryan, A., Iraeta Orbegozo, M., Mylopotamitaki, D., Wooller, M., Bataille,
615 C., Becerra-Valdivia, L., Chivall, D., Comeskey, D., Devière, T., Grayson, D.K.,
616 George, L., Harry, H., Alexandersen, V., Primeau, C., Erlandson, J., Rodrigues-
617 Carvalho, C., Reis, S., Bastos, M.Q.R., Cybulski, J., Vullo, C., Morello, F., Vilar,
618 M., Wells, S., Gregersen, K., Hansen, K.L., Lynnerup, N., Mirazón Lahr, M.,
619 Kjær, K., Strauss, A., Alfonso-Durruty, M., Salas, A., Schroeder, H., Higham, T.,
620 Malhi, R.S., Rasic, J.T., Souza, L., Santos, F.R., Malaspinas, A.-S., Sikora, M.,
621 Nielsen, R., Song, Y.S., Meltzer, D.J., Willerslev, E., 2018. Early human
622 dispersals within the Americas. *Science* 362, eaav2621.
623 <https://doi.org/10.1126/science.aav2621>

624 Narasimhan, V.M., Patterson, N., Moorjani, P., Rohland, N., Bernardos, R., Mallick, S.,
625 Lazaridis, I., Nakatsuka, N., Olalde, I., Lipson, M., Kim, A.M., Olivieri, L.M.,
626 Coppa, A., Vidale, M., Mallory, J., Moiseyev, V., Kitov, E., Monge, J., Adamski,
627 N., Alex, N., Broomandkhoshbacht, N., Candilio, F., Callan, K., Cheronet, O.,
628 Culleton, B.J., Ferry, M., Fernandes, D., Freilich, S., Gamarra, B., Gaudio, D.,
629 Hajdinjak, M., Harney, E., Harper, T.K., Keating, D., Lawson, A.M., Mah, M.,
630 Mandl, K., Michel, M., Novak, M., Oppenheimer, J., Rai, N., Sirak, K., Slon, V.,
631 Stewardson, K., Zalzal, F., Zhang, Z., Akhatov, G., Bagashev, A.N., Bagnera,
632 A., Baitanayev, B., Bendezu-Sarmiento, J., Bissembaev, A.A., Bonora, G.L.,
633 Charginov, T.T., Chikisheva, T., Dashkovskiy, P.K., Derevianko, A., Dobeš, M.,
634 Douka, K., Dubova, N., Duisengali, M.N., Enshin, D., Epimakhov, A., Fribus,
635 A.V., Fuller, D., Goryachev, A., Gromov, A., Grushin, S.P., Hanks, B., Judd, M.,
636 Kazizov, E., Khokhlov, A., Krygin, A.P., Kupriyanova, E., Kuznetsov, P.,
637 Luiselli, D., Maksudov, F., Mamedov, A.M., Mamirov, T.B., Meiklejohn, C.,
638 Merrett, D.C., Micheli, R., Mochalov, O., Mustafokulov, S., Nayak, A., Pettener,
639 D., Potts, R., Razhev, D., Rykun, M., Sarno, S., Savenkova, T.M., Sikhymbaeva,
640 K., Slepchenko, S.M., Soltobaev, O.A., Stepanova, N., Svyatko, S., Tabaldiev, K.,
641 Teschler-Nicola, M., Tishkin, A.A., Tkachev, V.V., Vasilyev, S., Velemínský, P.,
642 Voyakin, D., Yermolayeva, A., Zahir, M., Zubkov, V.S., Zubova, A., Shinde,
643 V.S., Lalueza-Fox, C., Meyer, M., Anthony, D., Boivin, N., Thangaraj, K.,

644 Kennett, D.J., Frachetti, M., Pinhasi, R., Reich, D., 2019. The formation of human
645 populations in South and Central Asia. *Science* 365, eaat7487.
646 <https://doi.org/10.1126/science.aat7487>

647 Olalde, I., Brace, S., Allentoft, M.E., Armit, I., Kristiansen, K., Booth, T., Rohland, N.,
648 Mallick, S., Szécsényi-Nagy, A., Mittnik, A., Altena, E., Lipson, M., Lazaridis, I.,
649 Harper, T.K., Patterson, N., Broomandkoshbacht, N., Diekmann, Y., Faltyskova,
650 Z., Fernandes, D., Ferry, M., Harney, E., de Knijff, P., Michel, M., Oppenheimer,
651 J., Stewardson, K., Barclay, A., Alt, K.W., Liesau, C., Ríos, P., Blasco, C.,
652 Miguel, J.V., García, R.M., Fernández, A.A., Bánffy, E., Bernabò-Brea, M.,
653 Billoin, D., Bonsall, C., Bonsall, L., Allen, T., Büster, L., Carver, S., Navarro,
654 L.C., Craig, O.E., Cook, G.T., Cunliffe, B., Denaire, A., Dinwiddy, K.E.,
655 Dodwell, N., Ernée, M., Evans, C., Kuchařík, M., Farré, J.F., Fowler, C.,
656 Gazenbeek, M., Pena, R.G., Haber-Uriarte, M., Haduch, E., Hey, G., Jowett, N.,
657 Knowles, T., Massy, K., Pfrengle, S., Lefranc, P., Lemerrier, O., Lefebvre, A.,
658 Martínez, C.H., Olmo, V.G., Ramírez, A.B., Maurandi, J.L., Majó, T., McKinley,
659 J.I., McSweeney, K., Mende, B.G., Mod, A., Kulcsár, G., Kiss, V., Czene, A.,
660 Patay, R., Endrődi, A., Köhler, K., Hajdu, T., Szeniczey, T., Dani, J., Bernert, Z.,
661 Hoole, M., Cheronet, O., Keating, D., Velemínský, P., Dobeš, M., Candilio, F.,
662 Brown, F., Fernández, R.F., Herrero-Corral, A.-M., Tusa, S., Carnieri, E., Lentini,
663 L., Valenti, A., Zanini, A., Waddington, C., Delibes, G., Guerra-Doce, E., Neil,
664 B., Brittain, M., Luke, M., Mortimer, R., Desideri, J., Besse, M., Brücken, G.,
665 Furmanek, M., Hałaszkó, A., Mackiewicz, M., Rapiński, A., Leach, S., Soriano,
666 I., Lillios, K.T., Cardoso, J.L., Pearson, M.P., Włodarczak, P., Price, T.D., Prieto,
667 P., Rey, P.-J., Risch, R., Rojo Guerra, M.A., Schmitt, A., Serralongue, J., Silva,
668 A.M., Smrčka, V., Vergnaud, L., Zilhão, J., Caramelli, D., Higham, T., Thomas,
669 M.G., Kennett, D.J., Fokkens, H., Heyd, V., Sheridan, A., Sjögren, K.-G.,
670 Stockhammer, P.W., Krause, J., Pinhasi, R., Haak, W., Barnes, I., Lalueza-Fox,
671 C., Reich, D., 2018. The Beaker phenomenon and the genomic transformation of
672 northwest Europe. *Nature* 555, 190–196. <https://doi.org/10.1038/nature25738>

673 Olalde, I., Mallick, S., Patterson, N., Rohland, N., Villalba-Mouco, V., Silva, M., Dulias,
674 K., Edwards, C.J., Gandini, F., Pala, M., Soares, P., Ferrando-Bernal, M.,
675 Adamski, N., Broomandkoshbacht, N., Cheronet, O., Culleton, B.J., Fernandes,
676 D., Lawson, A.M., Mah, M., Oppenheimer, J., Stewardson, K., Zhang, Z.,
677 Jiménez Arenas, J.M., Toro Moyano, I.J., Salazar-García, D.C., Castanyer, P.,
678 Santos, M., Tremoleda, J., Lozano, M., García Borja, P., Fernández-Eraso, J.,
679 Mujika-Alustiza, J.A., Barroso, C., Bermúdez, F.J., Viguera Mínguez, E., Burch,
680 J., Coromina, N., Vivó, D., Cebrià, A., Fullola, J.M., García-Puchol, O., Morales,
681 J.I., Oms, F.X., Majó, T., Vergès, J.M., Díaz-Carvajal, A., Ollich-Castanyer, I.,
682 López-Cachero, F.J., Silva, A.M., Alonso-Fernández, C., Delibes de Castro, G.,
683 Jiménez Echevarría, J., Moreno-Márquez, A., Pascual Berlanga, G., Ramos-
684 García, P., Ramos-Muñoz, J., Vijande Vila, E., Aguilera Arzo, G., Esparza
685 Arroyo, Á., Lillios, K.T., Mack, J., Velasco-Vázquez, J., Waterman, A., Benítez
686 de Lugo Enrich, L., Benito Sánchez, M., Agustí, B., Codina, F., de Prado, G.,
687 Estalrich, A., Fernández Flores, Á., Finlayson, C., Finlayson, G., Finlayson, S.,
688 Giles-Guzmán, F., Rosas, A., Barciela González, V., García Atiénzar, G.,
689 Hernández Pérez, M.S., Llanos, A., Carrión Marco, Y., Collado Beneyto, I.,

690 López-Serrano, D., Sanz Tormo, M., Valera, A.C., Blasco, C., Liesau, C., Ríos,
 691 P., Daura, J., de Pedro Michó, M.J., Diez-Castillo, A.A., Flores Fernández, R.,
 692 Francès Farré, J., Garrido-Pena, R., Gonçalves, V.S., Guerra-Doce, E., Herrero-
 693 Corral, A.M., Juan-Cabanilles, J., López-Reyes, D., McClure, S.B., Merino Pérez,
 694 M., Oliver Foix, A., Sanz Borràs, M., Sousa, A.C., Vidal Encinas, J.M., Kennett,
 695 D.J., Richards, M.B., Werner Alt, K., Haak, W., Pinhasi, R., Lalueza-Fox, C.,
 696 Reich, D., 2019. The genomic history of the Iberian Peninsula over the past 8000
 697 years. *Science* 363, 1230–1234. <https://doi.org/10.1126/science.aav4040>
 698 Pinhasi, R., Fernandes, D., Sirak, K., Novak, M., Connell, S., Alpaslan-Roodenberg, S.,
 699 Gerritsen, F., Moiseyev, V., Gromov, A., Raczky, P., Anders, A., Pietrusewsky,
 700 M., Rollefson, G., Jovanovic, M., Trinhhoang, H., Bar-Oz, G., Oxenham, M.,
 701 Matsumura, H., Hofreiter, M., 2015. Optimal Ancient DNA Yields from the Inner
 702 Ear Part of the Human Petrous Bone. *PLOS ONE* 10, e0129102.
 703 <https://doi.org/10.1371/journal.pone.0129102>
 704 Posth, C., Nakatsuka, N., Lazaridis, I., Skoglund, P., Mallick, S., Lamnidis, T.C.,
 705 Rohland, N., Nägele, K., Adamski, N., Bertolini, E., Broomandkoshbacht, N.,
 706 Cooper, A., Culleton, B.J., Ferraz, T., Ferry, M., Furtwängler, A., Haak, W.,
 707 Harkins, K., Harper, T.K., Hünemeier, T., Lawson, A.M., Llamas, B., Michel, M.,
 708 Nelson, E., Oppenheimer, J., Patterson, N., Schiffels, S., Sedig, J., Stewardson,
 709 K., Talamo, S., Wang, C.-C., Hublin, J.-J., Hubbe, M., Harvati, K., Nuevo
 710 Delaunay, A., Beier, J., Francken, M., Kaulicke, P., Reyes-Centeno, H.,
 711 Rademaker, K., Trask, W.R., Robinson, M., Gutierrez, S.M., Prufer, K.M.,
 712 Salazar-García, D.C., Chim, E.N., Müller Plumm Gomes, L., Alves, M.L., Liryo,
 713 A., Inglez, M., Oliveira, R.E., Bernardo, D.V., Barioni, A., Wesolowski, V.,
 714 Scheifler, N.A., Rivera, M.A., Plens, C.R., Messineo, P.G., Figuti, L., Corach, D.,
 715 Scabuzzo, C., Eggers, S., DeBlasis, P., Reindel, M., Méndez, C., Politis, G.,
 716 Tomasto-Cagigao, E., Kennett, D.J., Strauss, A., Fehren-Schmitz, L., Krause, J.,
 717 Reich, D., 2018. Reconstructing the Deep Population History of Central and
 718 South America. *Cell* 175, 1185-1197.e22.
 719 <https://doi.org/10.1016/j.cell.2018.10.027>
 720 Rasmussen, M., Anzick, S.L., Waters, M.R., Skoglund, P., DeGiorgio, M., Stafford,
 721 T.W., Rasmussen, S., Moltke, I., Albrechtsen, A., Doyle, S.M., Poznik, G.D.,
 722 Gudmundsdottir, V., Yadav, R., Malaspina, A.-S., V, S.S.W., Allentoft, M.E.,
 723 Cornejo, O.E., Tambets, K., Eriksson, A., Heintzman, P.D., Karmin, M.,
 724 Korneliussen, T.S., Meltzer, D.J., Pierre, T.L., Stenderup, J., Saag, L., Warmuth,
 725 V.M., Lopes, M.C., Malhi, R.S., Brunak, S., Sicheritz-Ponten, T., Barnes, I.,
 726 Collins, M., Orlando, L., Balloux, F., Manica, A., Gupta, R., Metspalu, M.,
 727 Bustamante, C.D., Jakobsson, M., Nielsen, R., Willerslev, E., 2014. The genome
 728 of a Late Pleistocene human from a Clovis burial site in western Montana. *Nature*
 729 506, 225–229. <https://doi.org/10.1038/nature13025>
 730 Reich, D., 2018. *Who We Are and How We Got Here: Ancient DNA and the New*
 731 *Science of the Human Past*. Pantheon, New York.
 732 Reich, D., Green, R.E., Kircher, M., Krause, J., Patterson, N., Durand, E.Y., Viola, B.,
 733 Briggs, A.W., Stenzel, U., Johnson, P.L.F., Maricic, T., Good, J.M., Marques-
 734 Bonet, T., Alkan, C., Fu, Q., Mallick, S., Li, H., Meyer, M., Eichler, E.E.,
 735 Stoneking, M., Richards, M., Talamo, S., Shunkov, M.V., Dereviako, A.P.,

736 Hublin, J.-J., Kelso, J., Slatkin, M., Pääbo, S., 2010. Genetic history of an archaic
737 hominin group from Denisova Cave in Siberia. *Nature* 468, 1053–1060.
738 <https://doi.org/10.1038/nature09710>

739 Saag, Lehti, Laneman, M., Varul, L., Malve, M., Valk, H., Razzak, M.A., Shirobokov,
740 I.G., Khartanovich, V.I., Mikhaylova, E.R., Kushniarevich, A., Scheib, C.L.,
741 Solnik, A., Reisberg, T., Parik, J., Saag, Lauri, Metspalu, E., Rootsi, S.,
742 Montinaro, F., Remm, M., Mägi, R., D’Atanasio, E., Crema, E.R., Díez-del-
743 Molino, D., Thomas, M.G., Kriiska, A., Kivisild, T., Villems, R., Lang, V.,
744 Metspalu, M., Tambets, K., 2019. The Arrival of Siberian Ancestry Connecting
745 the Eastern Baltic to Uralic Speakers further East. *Current Biology*
746 S0960982219304245. <https://doi.org/10.1016/j.cub.2019.04.026>

747 Skoglund, P., Posth, C., Sirak, K., Spriggs, M., Valentin, F., Bedford, S., Clark, G.R.,
748 Reepmeyer, C., Petchey, F., Fernandes, D., Fu, Q., Harney, E., Lipson, M.,
749 Mallick, S., Novak, M., Rohland, N., Stewardson, K., Abdullah, S., Cox, M.P.,
750 Friedlaender, F.R., Friedlaender, J.S., Kivisild, T., Koki, G., Kusuma, P.,
751 Merriwether, D.A., Ricaut, F.-X., Wee, J.T.S., Patterson, N., Krause, J., Pinhasi,
752 R., Reich, D., 2016. Genomic insights into the peopling of the Southwest Pacific.
753 *Nature* 538, 510–513. <https://doi.org/10.1038/nature19844>

754 Taylor, R.E., Bar-Yosef, O., 2014. Radiocarbon dating: an archaeological perspective,
755 Second edition. ed. Left Coast Press, Inc, Walnut Creek, California.

756 van de Loosdrecht, M., Bouzouggar, A., Humphrey, L., Posth, C., Barton, N., Aximu-
757 Petri, A., Nickel, B., Nagel, S., Talbi, E.H., El Hajraoui, M.A., Amzazi, S.,
758 Hublin, J.-J., Pääbo, S., Schiffels, S., Meyer, M., Haak, W., Jeong, C., Krause, J.,
759 2018. Pleistocene North African genomes link Near Eastern and sub-Saharan
760 African human populations. *Science* 360, 548–552.
761 <https://doi.org/10.1126/science.aar8380>
762
763